OBTAINING AVERAGE CRUSTAL AND UPPERMOST MANTLE PROPERTIES FOR PLANETARY MODELS OF MARS. D. Kim[1], S. C. Stähler[1], C. Boehm[1], V. Lekic[2], D. Giardini[1], M. Wieczorek[3], S. Ceylan[1], J. F. Clinton[4], A. Khan[1], A. C. Plesa[5], M. P. Panning[6], P. Lognonné[7] and W. B. Banerdt[6], [1]Institute of Geophysics, ETH Zurich, Switzerland (doyeon.kim@erdw.ethz.ch), [2]Department of Geology, University of Maryland, College Park, MD, USA, [3]Université Côte d'Azur, Observatoire de la Côte d'Azur, CNRS, Laboratoire Lagrange, Nice, France, [4]Swiss Seismological Service, ETH Zurich, Switzerland, [5]Institute of Planetary Research, German Aerospace Center (DLR), Berlin, Germany, [6]Jet Propulsion Laboratory, California Institute of Technology, Pasadena, CA, USA, [7]Université Paris Cité, Institut de physique du globe de Paris, CNRS, Paris, France.

Overview: After more than 4 Earth years (∼1450 sols) of operations on the martian surface monitoring the planet's ground vibrations, the InSight's seismometer is now retired. Throughout the mission, analyses of body waves from marsquakes and impacts have led to important discoveries about the planet's interior structure of the crust, mantle, and core [1-5]. Recent detection of surface waves, together with gravimetric modeling enabled the characterization of crustal structure variations away from the InSight landing site and showed that average crustal velocity and density structure is similar between the northern lowlands and the southern highlands [6-7].

These new constraints obtained by surface wave measurements provide an important opportunity to refine and verify our previous radially symmetric models of the planet's interior structure. As part of this effort, we obtain the average crustal and uppermost mantle velocities of Mars using Rayleigh waves orbiting the planet multiple times.

These higher-orbit Rayleigh wave observables independently constrain the average crustal and uppermost mantle velocities, and crustal thickness, which are found to be consistent with previous InSight studies. Successful incorporating of these velocity constraints into the existing joint inversion framework used for modeling body wave travel times [8], geophysical [9], and geodynamic parameters [10] will improve the current reference 1D interior models of Mars.

Higher-orbit Rayleigh waves in S1222a record: The largest event detected during the mission is marsquake S1222a (M_W^{Ma}4.6). Its waveform contains Rayleigh and Love waves, overtones, and multiple-orbit Rayleigh waves up to R7 (Figure 1A-B). Group velocities of R2-R7 are measured by using Nth-root stacking of vertical component data across different periods. Two distinctive group velocities of 2.88 km/s and 3.81 km/s for R2-R7 in S1222a are observed at 30 s and 85 s periods, respectively (Figure 1C). Unlike typical, smoothly-varying surface wave dispersion curves, the observed group velocities show apparent jumps in velocity, which we show to be due to large lateral variation of crustal properties along the paths.

3D wavefield simulation of higher-orbit Rayleigh waves: Previously, we have reported little deviation in travel times for R1-R3 between the great-circle propagation and the ray theoretical path based on 3D crustal models of Mars [7]. To obtain more realistic 3D sensitivity kernels for higher-orbit surface waves beyond R3, we perform 3D wavefield simulations using the spectral-element method [11]. We replace the crust in the 1-D reference velocity model of KKS21 [4] by [7] and extrapolate globally based on the crustal thickness model constrained by gravity data [12].

Our preliminary synthetic record of S1222a reproduces Rayleigh wave group velocities observed in the data with the abruptness of dispersion curves that has been caused by the 3D crustal effect (Figure 1B). While average crustal velocity in the short-period stack is consistent with that of the 3D synthetics, we find average uppermost mantle velocity in the long-period stack is 12% larger than the values obtained by our synthetics (Figure 1C-D).

This result illustrates that the uppermost mantle velocities in the previously obtained interior models of Mars are not fully representative for all source-receiver paths. We are currently computing 3D sensitivity kernels for R2-R7 to quantify the volumetric sensitivities for the observed group velocities in S1222a and to constrain globally-averaged crust and uppermost mantle velocities.

Average crustal properties of Mars: The expected outcome from this study will provide the posterior distributions of average crustal and uppermost mantle shear velocity (V_S) and Moho thickness on Mars that better represent global variations. Accurate knowledge of structure along diverse source-receiver paths is important for locating and constraining source mechanisms of marsquakes. Therefore, our surface-wave constrained models provide both an important opportunity to constrain a globally-representative reference model for Mars and to improve understanding of seismo-tectonic environments on Mars.

Acknowledgments: We acknowledge NASA, CNES, their partner agencies and institutions (UKSA, SSO, DLR, JPL, IPGP-CNRS, ETHZ, IC and MPS-MPG) and the flight operations team at JPL, SISMOC,

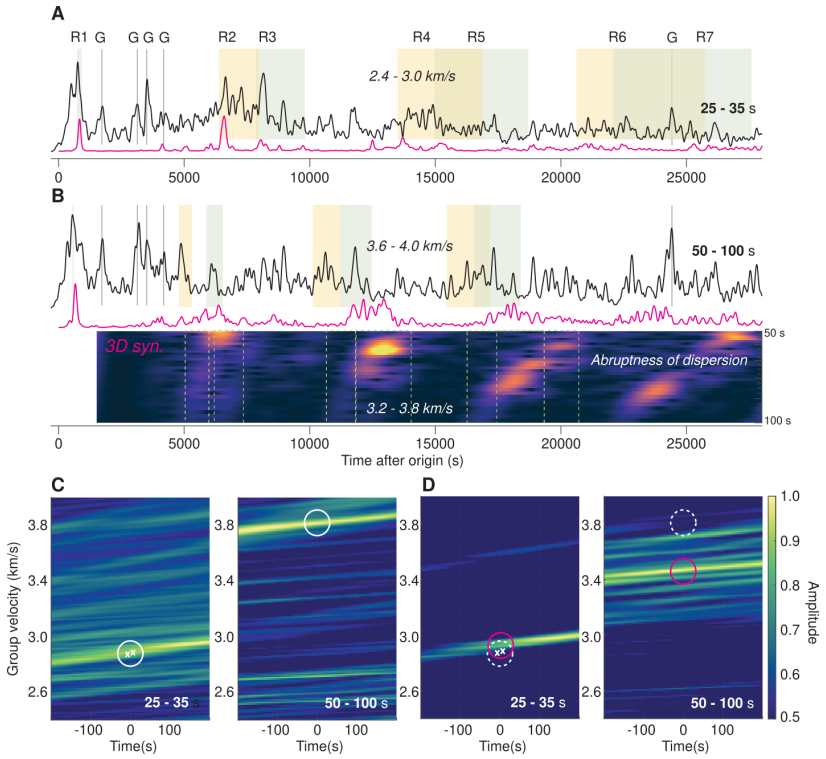

Figure 1: Vertical component envelopes of the S1222a deglitched waveform filtered between (A) 25-35 s and (B) 50-100 s periods. Shaded areas indicate the predicted time windows of R1-R7 arrivals base on the group velocities ranging from 2.4-3.0 km/s to 3.6-4.0 km/s for short- and long-period data, respectively. Glitches are shown by gray lines. Envelopes in magenta are based on 3D wavefield simulations. Abruptness of dispersion for >R3 is visible in the spectrogram of the vertical component synthetic waveform. Variation in amplitudes for R3, R5, R7 vs. R2, R4, R6 likely result from (de)focusing by lateral variations in velocity [13]. Dashed lines are the group velocity prediction windows for 3.2-3.8 km/s. Group velocity measurements of R2-R7 are obtained by Nth-root stacking of data across different periods shown in (A-B) for (C) data and (D) synthetics.

MSDS IRIS-DMC and PDS for delivery of SEIS data and operating the InSight mission.

References: [1] Knapmeyer-Endrun B. et al. (2021) Science, 373, 438–443. [2] Kim D. et al. (2021) JGR-Planets, 126 (11), e2021JE006983. [3] Khan A. et al. (2021) Science, 373, 434–438. [4] Stähler S. C. et al. (2021) Science, 373, 443–448. [5] Khan A. et al. (2022) EPSL, 578, 117330. [6] Kim D. et al. (2022) Science, 378, 417-421. [7] Kim D. et al. (2022) GRL, e2022GL101666. [8] InSight Marsquake Service (2023) Mars Seismic Catalogue, InSight Mission; v13 2023-01-01, ETHZ, IPGP, JPL, ICL, Univ. Bristol, doi: 10.12686/a19. [9] Duran C. et al. (2022) PEPI, 325, 106851. [10] Drilleau D. et al. (2022) JGR-Planets, 127(9), e2021JE007067. [11] Afanasiev M. et al. (2019) GJI, 216(3), 1675-16922. [12] Wieczorek M. et al. (2022) JGR-Planets, 127(5), e2022JE007298. [13] Romanowicz (1987) GJI, 90(1), 75-100.